J Therm Anal Calorim
DOI 10.1007/s10973-016-6004-7

The investigations of thermal behavior, kinetic analysis, and biological activity of trinuclear complexes prepared ONNO-type Schiff bases with nitrito and nitrato μ-bridges

Nurcan Acar[1] · Orhan Atakol[1] · Şaziye Betül Sopacı[2] · Demet Cansaran Duman[3] · Ingrid Svoboda[4] · Sevi Öz[2]

Received: 3 July 2016 / Accepted: 25 November 2016

Abstract By using bis-*N*,*N*′(salicylidene)-1,3-diaminopropane and reduced form of this ligand bis-*N*,*N*′(2-hydroxybenzylidene)-1,3-diaminopropane, we prepared eight trinuclear complexes in the core form of Ni^{II}–Ni^{II}–Ni^{II} and Ni^{II}–Cu^{II}–Ni^{II}. Complexes have been characterized with element analysis, IR spectroscopy and NMR spectroscopy methods and also investigated with Thermogravimetry (TG). It was observed that thermal characteristics of the complexes prepared by the reduced form of Schiff base are different from complexes prepared by the Schiff base. According to TG, two thermal reactions between 120 and 180 °C endothermic separation of coordinative dimethylformamide molecules and then around 300 °C exothermic decomposition of molecule were observed for Schiff base-prepared complexes. On the other hand, the complexes resulted from reduced Schiff base reactions were shown decomposed around 250–270 °C by exothermic thermal reaction. Kinetic parameters of decompositions were determined by isothermal and non-isothermal kinetic methods, Coats–Redfern (CR), Ozawa, Ozawa–Flynn–Wall (OFW) and Kissenger–Akahira–Sunose (KAS). Departing from these values, thermodynamic parameters were calculated and the results were interpreted. It was concluded that the complexes prepared with reduced Schiff bases are more strained structures. Biological activities of these complexes were also inspected, and antibacterial and antifungal activities were tested against four different bacterial strains (*E. coli, P. aureginosa*, *S. aureus and E. feacalis*) and a fungus species (*C. albicans*).

Keywords Reduced Schiff base · Trinuclear complex · Isothermal and non-isothermal kinetic · Ozawa method · OFW · Coats–Redfern method

Introduction

Bis-*N*,*N*′(salicylidene)-1,3-diaminopropane (LH_2) and their derivatives are very inclined ligands to give polynuclear complexes; since 1990, there are number of homo and hetero polynuclear complexes prepared with these ligands and were reported in the literature [1–25]. During the formation of these polynuclear complexes, acetate [2–10, 21, 22], chloride [11], azide, formate [15–18], benzoate [18], nitrite [19] and nitrate [17, 20] anions constitute μ-bridge. The structure of the coordination sphere of the terminal and central metal ions is different in trinuclear complexes. Terminal metal ions are located in between two nitrogen of LH_2 ligand, two phenolic and one solvent molecule oxygen and anion in the environment (acetate, format, benzoate, nitrite or nitrate) having a coordination sphere as N_2O_4 form; however, central metal ions formed coordination between four phenolic oxygen and oxygen of anion in the environment and have O_6 coordination sphere [5–10]. Trinuclear complexes can be prepared by two different ways by using Schiff bases.

First of them is template synthesis method. According to this method, ligand, metal ions and combining anion are

✉ Sevi Öz
sevioz@hotmail.com

1 Department of Chemistry, Faculty of Science, Ankara University, 06100 Ankara, Turkey

2 Department of Chemistry, Faculty of Science and Arts, Ahi Evran University, 40100 Kırşehir, Turkey

3 Biotechnology Institute, Ankara University, 06100 Ankara, Turkey

4 Strukturforschung, FB Materialwissenschaft, TU- Darmstadt, Petersenstrasse 23, 12 64287 Darmstadt, Germany

Published online: 20 December 2016

reacted in a proper solvent sample such as DMF, DMSO or in dioxane media and trinuclear complexes are obtained as a result, [21–25].

The second method consists of two steps. LH_2 and mononuclear NiL complex could be formed by interacting nickel salts, and then, trinuclear complex could be synthesized with this mononuclear complex in DMF, DMSO or dioxane as solvent, [16, 23].

Schiff bases could be easily reduced in amphiprotic solvents with the help of $NaBH_4$ [21–23]. In consequence of reducing imine, nitrogen groups could be transformed into secondary amine groups and phenol–amine ligands are obtained from phenol–imine-type ligands, Fig. 1.

So far, it is not possible to prepare a mononuclear complex with reduced ligands and a NiL^H stoichiometry complex was not isolated. For that reason, two-step synthesis of these complexes with reduced Schiff bases is not possible. By using reduced Schiff bases, trinuclear complexes were obtained by template synthesis, [21–25].

Taking into account iminic nitrogens are converted to amines, electron density of the nitrogens should increase in the reduced ligand. Therefore, easier synthesis of mononuclear Ni(II) complexes was expected. There are many proper dealings related with the complex formation using the above Schiff base compound and its reduced states. Structural analysis of the Schiff base complex reveals 10°–18° angle between the metal ion-two iminic nitrogen and two iminic nitrogen—bonded carbon atoms planes. In the reduced state, this angle is 35°–40° [26, 27]. Ideally, this angle is around 62°. Under these circumstances, the reduced Schiff base complex is expected to be more stable, but a stable mononuclear complex was not isolated. To explain this, thermogravimetrical analysis was employed and many reports have been published related with TG analysis of trinuclear complexes prepared with Schiff bases [18, 28].

In these researches, it was clearly observed that DMF molecules connected to terminal groups were separated from structure as thermally and mass losses gave significant results in characterization of complexes. But this mass loss related to the DMF's separation was not observed in reduced Schiff bases. In order to explain this situation, by using nitrite and nitrate-bridged anions with LH_2 ligand four complexes and with L^HH_2 ligands, four trinuclear complexes were prepared by template synthesis and examined by thermogravimetry. In these complexes, nitrite and nitrate auxiliary anions were used as μ-bridge. There are some examples for trinuclear complexes prepared by using these anions in the literature, and in these reports, structures of μ-bridges made by nitrite and nitrate anions were determined [15–18, 20]. While nitrite anion is connected to terminal metal ion over oxygen, it is also connected to central metal ion over nitrogen ion; nitrate anion is connected to terminal metal ion by oxygen and connected to central metal ion with second oxygen. The complexes prepared in this study were not obtained as proper crystals, but a similar structure, which was prepared to show the coordination of the nitrate ion, is included in this study. This complex was prepared by bis-*N*,*N*′(2-hydroxyacetophenone)-1,3-propanediamine ($LACH_2$) and added to this study in order to show μ-bridges of nitrate ion. The total formulas of prepared complexes are shown below, and structures are shown in Fig. 2.

Complexes prepared by Schiff bases	
{[DMF·NiL·Cu$(NO_2)_2$·NiL·DMF]·1/2DMF}	(I)
{[DMF·NiL·Cu$(NO_3)_2$·NiL·DMF]·DMF}	(II)
[DMF·NiL·Ni$(NO_2)_2$·NiL·DMF]	(III)
{[DMF·NiL·Ni$(NO_3)_2$·NiL·DMF]·2DMF}	(IV)
{[DMF·NiLAC·Cu$(NO_3)_2$·NiLAC·DMF]·DMF}	(V)
Complexes prepared with reduced Schiff bases	
[DMF·NiL^H·Cu$(NO_2)_2$·NiL^H·DMF]	(VI)
[DMF·NiL^H·Cu$(NO_3)_2$·NiL^H·DMF]	(VII)
[DMF·NiL^H·Ni$(NO_2)_2$·NiL^H·DMF]	(VIII)
[DMF·NiL^H·Ni$(NO_3)_2$·NiL^H·DMF]	(IX)

To investigate the strain possibility of these two complex groups, we examined them by thermogravimetric methods. Although complexes in these two groups are in similar structures, their thermo gravimetric curves were significantly different from each other. Activation energy and other thermodynamic parameters were calculated by isothermal and non-isothermal thermokinetic methods and compared. Activation energy was expected to be smaller in strained complexes, for that reason more than one methods

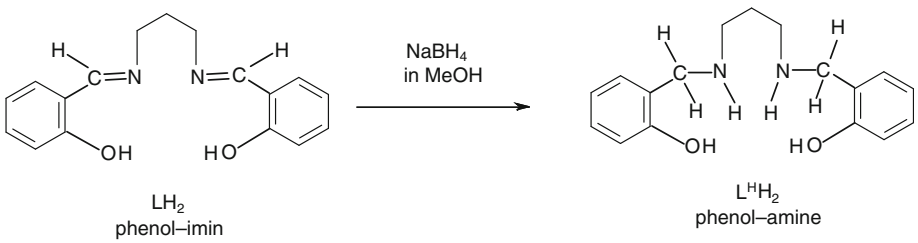

Fig. 1 Bis-*N*,*N*′(salicylidene)-1,3-propanediamine ligand's reduction reaction

Fig. 2 Structures of the prepared complexes

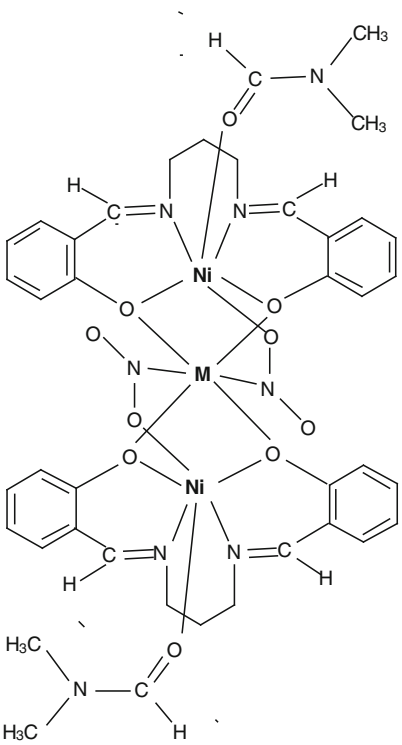

M=Cu(II) (I)
M=Ni(II) (III)

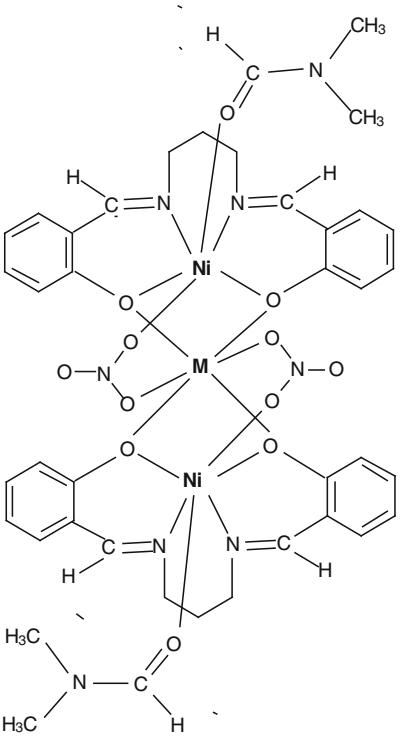

M=Cu(II) (II)
M=Ni(II) (IV)

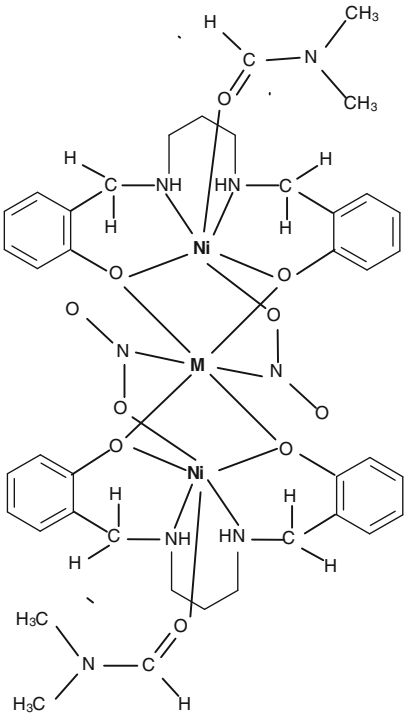

M=Cu(II) (VI)
M=Ni(II) (VIII)

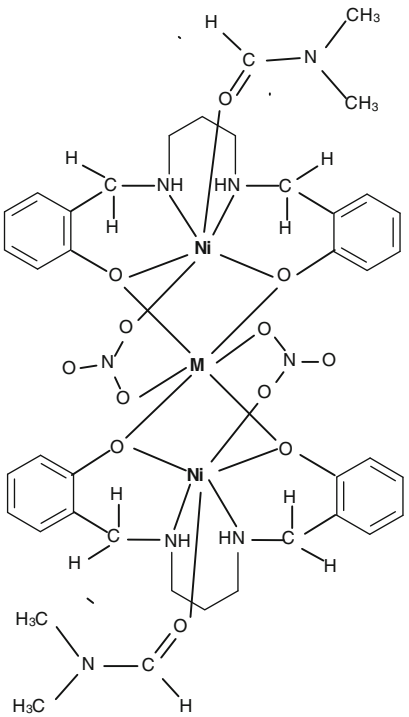

M=Cu(II) (VII)
M=Ni(II) (IX)

were used for calculation. Since it is possible to direct calculation of activation energy from thermo gravimetry curves employing Ozawa equation with a software, TA60 Version 2.01 of the device that we used, we preferred to use Ozawa method first [29, 30]. But due to explosive effects of nitrite and nitrate ions in higher temperatures, Ozawa method did not give any result for explosive exothermic reactions. For that reasons, non-isothermal kinetic methods Ozawa–Flynn–wall [31–35] and Kissenger–Akahira–Sunose [33–37], and as isothermal method Coast–Redfern [38, 39] were employed manually and thermokinetic results were obtained.

In the scope of this study, we also investigated biological activity of these complexes split into two different groups to compare the influence of different structures to their bioactivity, in consistent with the literature [38, 39]. Biological activities were determined on seven complexes. Behaviors of these complexes in DMF solution were assessed against gram-negative bacteria *Echericia coli* and *Pseudomonas aurogines* and against gram-positive bacteria *Staphilococcus aureus* and *Entorococcus feacalis* and a fungus *Candida albicans*. Minimum Inhibitory Concentration (MIC) values were determined for the eight complexes.

Experimental

Materials and apparatus

Used reactives were of Merck or Fluka brands, and they were used without further purification. In this study, Shimadzu Infinity FTIR spectrometer equipped with three reflectional ATR units was used for IR spectra with 4 cm^{-1} accuracy. The C, H and N analyses were performed on Eurovector 3018 C,H,N,S analyzer. Metal analyses were recorded on GBC Avanta PM Model atomic absorption spectrometer using FAAS mode. Complex (2–3 mg) was dissolved in 1 mL HNO3 (63%) with heating, diluted to 100 mL and given to nebulizer of atomic absorption spectroscopy for metal analysis. The mass spectra of the ligands were obtained by Shimadzu, 2010 plus with direct inlet (DI) unit with an electron impact ionizer. DI temperature was varied between 40 and 140 °C, and ionization was done with electrons with 70 eV energy. The NMR spectra were recorded on the Bruker Ultrashield 300 MHz NMR spectrometer. DMSO-d6 solution was the solvent. The thermogravimetric analyses were performed by Shimadzu DTG 60H. In thermogravimetric analyses, temperature was varied between 30 and 600 °C. These analyses were performed at 5, 10, 15, 20 and 25 °C/min rates and under N2 atmosphere in Pt pans. Calibration of the instrument was done with metallic In and Pb.

X-ray crystallography

A single crystal of [DMF·NiLAC·$Cu(NO_3)_2$·NiLAC·DMF] (complex V) was analyzed on an Oxford Diffraction Xcalibur single-crystal X-ray diffractometer with a sapphire CCD detector using Mo$K\alpha$ radiation ($\lambda = 0.71073$ A) operating in $\omega/2\theta$ scan mode. The unit-cell dimensions were determined and refined by using the angular settings of 25 automatically centered reflections in $2.85° \leq \theta \leq 228.24°$ range. The data of the complex V were collected at 100(2) K. The empirical absorption corrections were applied by the semi-empirical method via the CrysAlis CCD software [40]. The model was obtained from the results of the cell refinement, and the data reductions were carried out using the solution software SHELXL97 [41]. The structure of the complex V was determined by direct methods using the SHELXS-97 software implemented in the WinGX package [42]. Supplementary material for structure has been deposited with the Cambridge Crystallographic Data Center as CCDC no: 1481757 (deposit@ccdc.cam.ac.uk or http://www.ccdc.cam.ac.uk).

Biological activity of the complexes

Microbial strains

In the examined study, microorganisms were selected to include gram-positive bacteria (*Staphylococcus aureus* ATCC 25923 and *Enterococcus feacalis* RSKK 508), gram-negative bacteria (*Pseudomonas aeruginosa* ATCC 9027 and *E. Coli* ATCC 35218) and yeast (*Candida albicans* ATCC 10231). All the strains were stored at −20 °C in tryptic soya broth (TSB; Oxoid, Basingstoke, UK) with 20% glycerol.

The inocula of microorganism strains were prepared from an overnight culture for bacteria in Muller–Hinton agar, whereas Sabouraud agar was used for growing the fungi. The suspensions were adjusted to 0.5 McFarland for the turbidity (1×10^8 colony-forming units [CFU]/mL).

Antibacterial and antifungal test

The antimicrobial activity of the synthesized chemicals was assayed for the microdilution method, which determines the minimum inhibitory concentration (MIC) leading to the inhibition of bacterial growth. The composites in dispersion form were diluted 2–128 times with 100 mL of Mueller–Hinton broth inoculated with the tested bacteria at a concentration of $1° \times 10^5$ CFU/mL. The MIC was read after 24 h of incubation at 37 °C as the MIC of the tested substance that inhibited the growth of the bacterial strain. The dispersions were used in the form in which they had been prepared. Therefore, control bactericidal tests of solutions were

performed containing all the reaction components. Saturated stock solutions of the extracts were prepared in DMSO. Double serial dilutions were also prepared in the same solvent. Aliquots of the solutions (1 mL) were mixed with a fixed amount of molten Muller–Hinton agar at 45 °C to get the final concentrations. When the agar solidified, the plates were inoculated with 10 µL microbial suspension ($1° \times 10^6$ CFU/mL). The inoculated plates were incubated for 24 h at 35 °C for bacteria and for 48 h for the yeast. Each of the chemicals (0.312, 2.5, 1.25, 0.625 and 0.312 mg) were added in the plates. Positive controls for all microorganisms were prepared using 1 mL DMSO instead of an extract solution. After incubation, the plates were inspected visually. MIC was recorded as the lowest concentration at which no visible growth of the test pathogens was observed. The test was not considered valid unless the positive controls showed significant microbial growth. Standard antibiotic (amoxicillin) were used to control the sensitivity of the tested bacteria, and amphotericin B was used as controls against the tested fungi.

Preparation of the ligands

Preparation of N,N-bis (2-hydroxyphenylidene)-1,3-propanediamine (LH_2)

This Schiff base was prepared via condensation reaction in EtOH under hydrothermal conditions using 2-hydroxybenzaldehyde and 1,3-diaminopropane. 2-Hydroxybenzaldehyde (0.1 mol, 12.20 g) was dissolved in 120 cm^3 of warm EtOH; then, 0.05 mol (3.70 g) of 1,3-diaminopropane was added to this solution and heated up to the boiling point. After cooling, yellow crystals were filtered and dried in air. Yield: 90–95%, mp: 58 °C (determined by TG).

Elemental analysis for $C_{17}H_{18}N_2O_2$

Anal. Calcd. %: C 72.32; H 6.43; N 9.92.

Found %: C 71.95; H 6.33; N 10.09.

Important IR data (cm^{-1}): ν_{O-H}: 2627, $\nu_{C-H(Ar)}$: 3021–3019, $\nu_{C-H(Aliph)}$: 2929–2862, $\nu_{C=N}$: 1629, $\nu_{C=C(ring)}$: 1608, $\nu_{C-O(Phenol)}$: 1274–1151, $\delta_{C-H(Ar)}$: 762.

$\Lambda_{max} = 243$ nm, $\varepsilon = 7045$ dm^3 mol^{-1} cm^{-1} in DMSO, $\lambda_{max} = 242$ nm, $\varepsilon = 7865$ dm^3 mol^{-1} cm^{-1} in MeOH.

^{1}HNMR data in d_6-DMSO(δ, ppm): 13.51 (s) (O–H), 8.60 (s) (–CH=), 7.43 (d) (H_{Ar}), 7.32 (t) (H_{Ar}), 6.88 (t) (H_{Ar}), 3.68 (t) (N–CH_2–), 2.01 (p) (–CH_2–), Fig. 3.

^{13}CNMR data in d_6 DMSO(δ, ppm): 166.6 (–C=N), 161.1, 132.7, 132.1, 119.1, 118.9 116.9 (C_{Ar}), 58.5 (N–CH_2–), 31.9 (–CH_2–), Fig. 4.

MS *m/z*: 282 $[M]^+$, 161 $[HO–C_6H_4–CH=N–CH_2–CH_2–CH_2]^+$, 148 $[HO–C_6H_4–CH=N–CH_2–CH_2]^+$ (Basepeak), 134 $[HO–C_6H_4–CH=N–CH_2]^+$, 120 $[HO–C_6H_4–CH=N]^+$, 107 $[HO–C_6H_4–CH_2]^+$, 77 $[C_6H_5]^+$, Fig. 5.

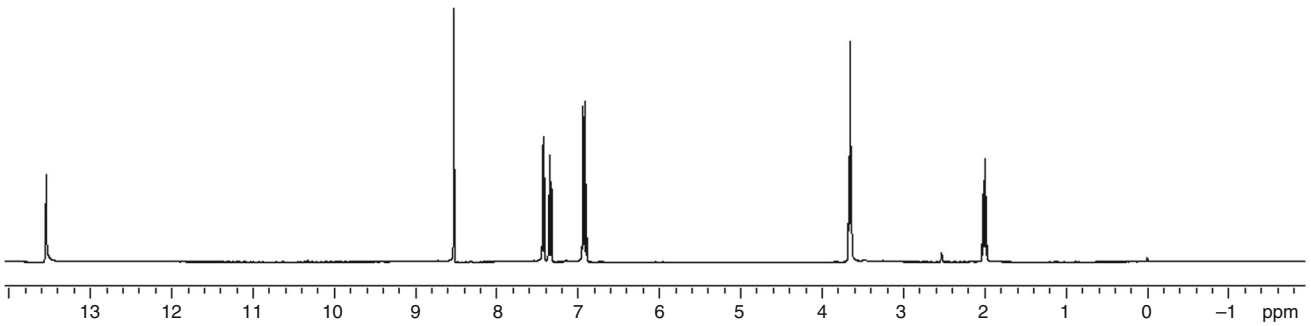

Fig. 3 ^{1}HNMR spectrum of LH_2

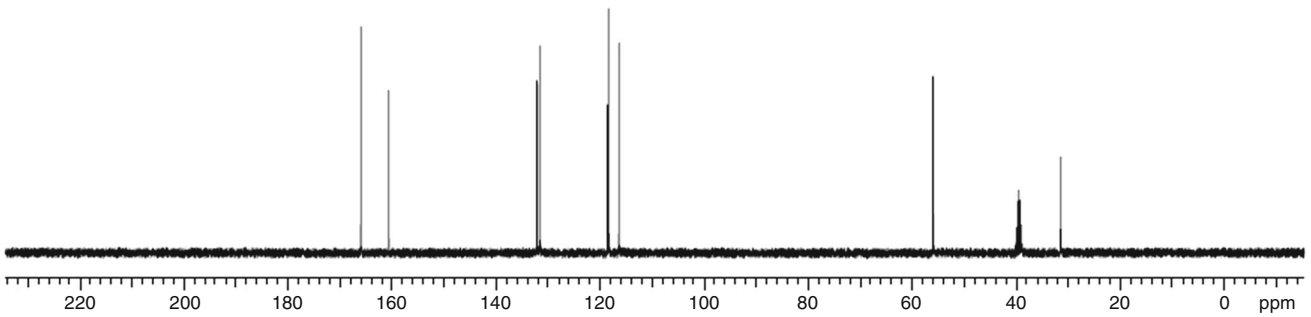

Fig. 4 ^{13}CNMR spectrum of LH_2

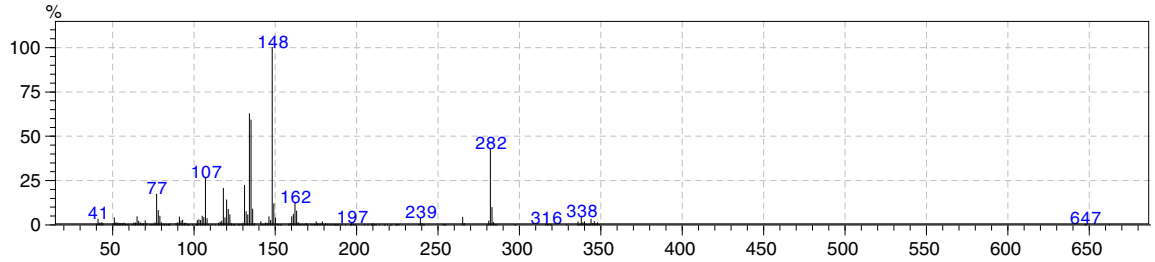

Fig. 5 MS fragments of LH_2 obtained using DI equipment

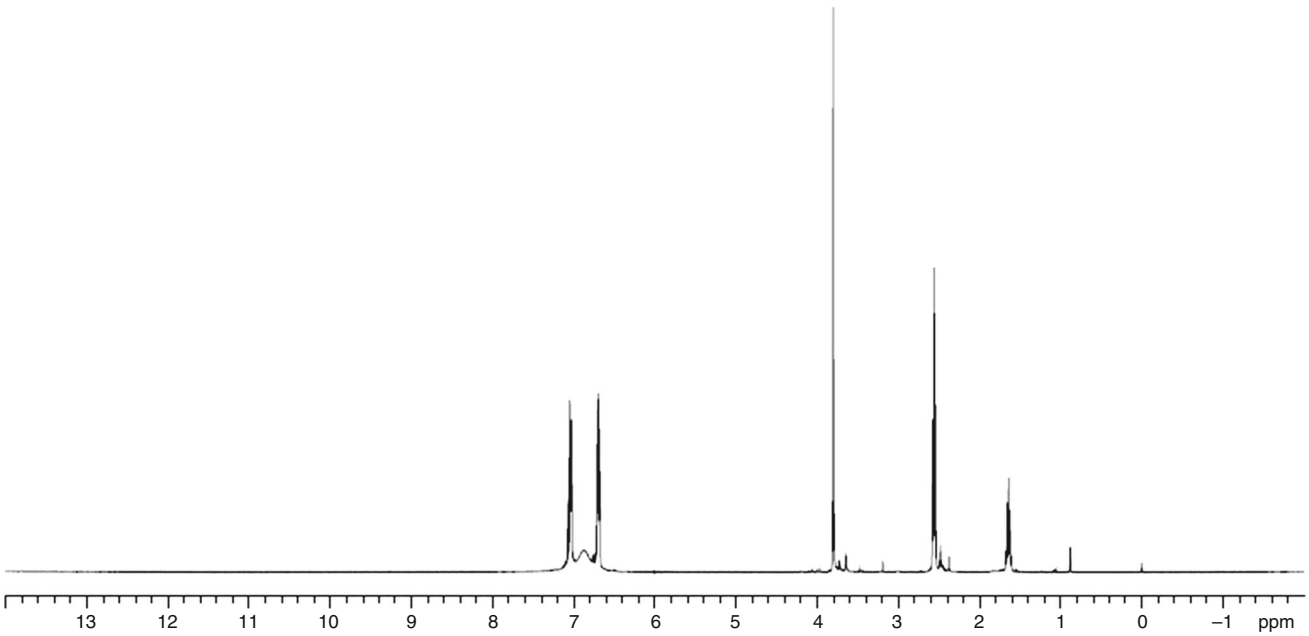

Fig. 6 ^{1}HNMR spectrum of $L^{H}H_2$

The phenolic hydrogens are observed at 13.51 ppm, the iminic hydrogens at 8.60 ppm and aromatic hydrogens at 7.43–6.68 ppm δ value in ^{1}HNMR spectrum. As expected the aliphatic hydrogens are seen at 3.68 and 2.01 ppm as triplet and pentet, respectively. On the other hand, in ^{13}CNMR spectrum are seen 9 different carbon atoms signals as expected. It is probable that the signal at 166 ppm observed is the signal of iminic carbon atom. The molecular mass of LH_2 Schiff base can be seen from the MS spectrum, and the signal at 282 *m/z* value observed is the molecular peak of LH_2.

Preparation of N,N-bis (2-hydroxybenzyl)-1,3-propanediamine ($L^{H}H_2$)

3.0 g of bis-*N*,*N*′(salicylidene)-1,3-propanediamine (LH_2) was dissolved in 70.0 cm^3 of MeOH by stirring and heating. This solution was heated up to 50 °C, and to this solution, solid $NaBH_4$ in small portions was added until colorless under strong mixing [31–34]. After 10 min of stirring, 300 cm^3 of ice water was added to it. The final mixture was left to stand for 24 h. After filtration, the white precipitate was air-dried. The product bis-*N*,*N*′(2-hydroxybenzyl)-1,3-propanediamine ($L^{H}H_2$) was recrystallized from hot EtOH:H_2O (2:1, v/v). Yield: 55–60%, mp: 107 °C.

Elemental analysis for $C_{17}H_{22}N_2O_2$

Anal. Calcd. %: C 71.30; H 7.74; N 8.01.

Found %: C 70.86; H 6.69; N 8.37.

Important IR data (cm^{-1}): ν_{N-H}: 3307, $\nu_{C-H(Ar)}$: 3055–3023, $\nu_{C-H(Aliph)}$: 2967–2823, $\nu_{C=C(ring)}$: 1606–595, $\nu_{CO(Phenol)}$: 1253–1099, $\delta_{C-H\ (Ar)}$: 752.

^{1}H NMR data in d_6-DMSO(δ, ppm): 7.12 (m), 6.67 (m), 6.83 (broad), 3.80 (m), 2.56 (m), 1.15 (m), Fig. 6.

^{13}C NMR data in d_6-DMSO (δ, ppm): 157.64, 128.43, 127.78, 124.61, 118.34, 115.39 (C_{Ar}), 50.80 (Ar–CH_2–N), 46.30 (HN–CH_2), 28.94 (CH_2–CH_2–CH_2), Fig. 7.

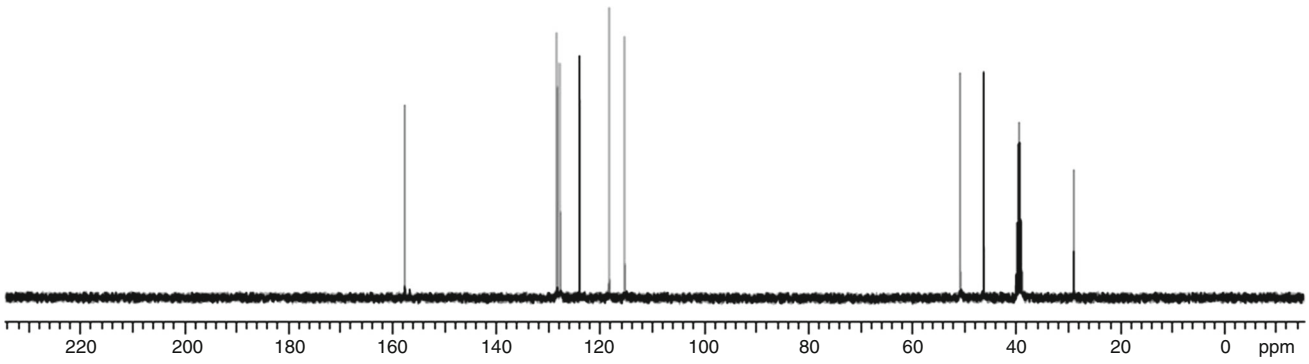

Fig. 7 ^{13}CNMR spectrum of $L^{H}H_2$

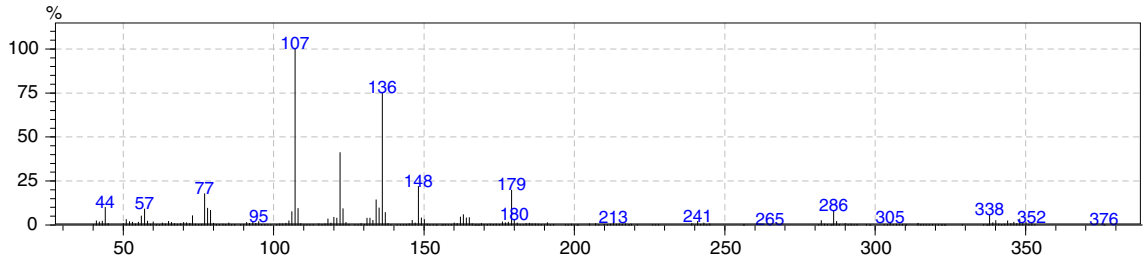

Fig. 8 MS fragments of $L^{H}H_2$ obtained using DI equipment

MS (*m/z*): 286 (molecular peak), 179 [HO–C_6H_4–CH_2–NH–CH_2–CH_2–CH_2–NH]$^+$, 163 [HO–C_6H_4–CH_2–NH–CH_2–CH_2–CH_2]$^+$, 150 [HO–C_6H_4–CH_2–NH–CH_2–CH_2]$^+$, 136 [HO–C_6H_4–CH_2–NH–CH_2]$^+$, 122 [HO–C_6H_4–CH_2–NH]$^+$, 107 [HO–C_6H_4–CH_2]$^+$ (base peak), 90 [C_6H_4–CH_2]$^+$, 77 [C_6H_5]$^+$, Fig. 8.

As shown in Fig. 6, a broad signal is observed between aromatic hydrogens signals. This signal is probably from amine hydrogens. But this signal was not observed in the diluted solution, whereas the signal of the phenolic hydrogens was seen at 13.2 ppm δ value in diluted solution. Due to the hydrogen bond formation, the signal of amine hydrogens is observed as a broad peak. Nine different C atoms signals are observed from the ^{13}CNMR spectrum. As the iminic double bond is transformed into a single bond, a signal at 166 ppm around is not observed, despite that to a new signal around 50 ppm. Weak molecular peak of the reduced Schiff base is observed at 286 *m/z* value from the mass spectrum.

Preparation of N,N-bis (2-hydroxyacetophenilidene)-1,3-propanediamine ($LACH_2$)

This Schiff base was obtained from 2-hydroxyacetophenone and 1,3-diaminopropane in EtOH under hydrothermal conditions using. 2-Hydroxyacetophenone (0.1 mol, 13.60 g) was dissolved in 150 cm^3 of warm EtOH; then, 0.05 mol (3.70 g) of 1,3-diaminopropane was added to this solution and heated up to the boiling point. After cooling, yellow crystals were filtered and dried in air. Yield: 94–96%, mp: 123.6 °C (determined by TG).

Elemental analysis

Expected % C: 73.52, H: 7.14, N: 9.02; Found % C: 73.09, H: 6.35, N: 8.82.

Important IR data (cm^{-1}): $\nu_{C–H(Ar)}$: 3036–3017, $\nu_{C–H(Aliph)}$: 2922–2944–2866, $\nu_{C=N}$: 1610, $\nu_{C=C(ring)}$: 1600, $\nu_{C–O(Phenol)}$: 1232–1159, $\delta_{C–H(Ar)}$: 754.

^{1}HNMR data in d$_6$-CH_3COCH_3: 13.68 (s), 8.71 (s), 7.45 (dd), 7.34 (td), 6.91 (t), 3.52 (t), 2.06 (p).

^{13}CNMR data in d-$CHCl_3$: *m/z:* 310 (MP), 193, 179, 164, 150, 136, 121 (BP), 107, 91.

Preparation of the complexes

As given above, trinuclear complexes can be synthesized by two different methods. The first method is known as template method. In this method, all reagents are reacted in the same solvent, Scheme 1.

The second method occurs in two steps: firstly, a mononuclear complex is obtained; then, trinuclear complex is synthesized in the second step, Scheme 2.

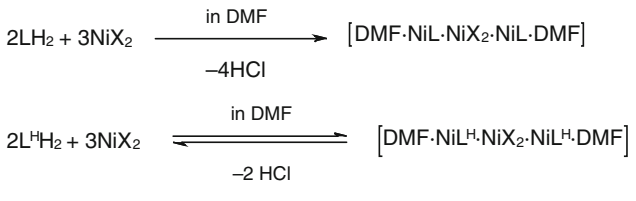

Scheme 1 Direct trinuclear complex formation with Schiff bases or reduced Schiff bases using template synthesis

Preparation of the Schiff base complexes (complex I–IV)

These complexes are synthesized according to Scheme 2 in two steps, previously was prepared mononuclear NiL complex from bis-*N*,*N*′(salicylidene)-1,3-propanediamine and $NiCl_2{\cdot}6H_2O$, secondly were prepared trinuclear complexes I–IV using this NiL complex.

Preparation of mononuclear NiL complex

NiL mononuclear complex was prepared as described according to the literature [43]. A quantity of 0.05 mol (14.1 g) bis-*N*,*N*′(salicylidene)-1,3-propanediamine was dissolved in 150 mL hot EtOH, and 10 mL concentrated ammonia was added to this solution. Then, a solution of 0.05 mol (11.80 g) $NiCl_2{\cdot}6H_2O$ in 50 mL hot water was added to this mixture. After setting, the solution was set aside for 2 h and light green precipitated was filtered and dried in a oven at 140 °C for 3–4 h.

Preparation of complexes I–IV

A quantity of 0.002 mol (0.680 g) of the complex NiL was dissolved in 50 mL DMF by heating until 110 °C. For complex I 0.001 mol (0.170 g) $CuCl_2{\cdot}2H_2O$ and 0.002 mol (0.140 g) $NaNO_2$, for complex II 0.001 mol (2.41 g) $Cu(NO_3)_2{\cdot}3H_2O$, for complex III 0.001 mol (0.236 g) $NiCl_2{\cdot}2H_2O$ and 0.002 mol (0.140 g) $NaNO_2$ and for complex IV 0.001 mol (0.291 g) $Ni(NO_3)_2{\cdot}6H_2O$ were dissolved in 30 mL water–MeOH mixture (v/v: %50–%50) using heating and mixed with the above solution. The resulting mixture was set aside for 3–4 days in air. After this period, the precipitated crystals products were filtered and dried in air. The analytical results of the complexes synthesized are given below.

Complex I, [DMF·NiL·Cu(NO$_2$)$_2$·NiL·DMF] ($C_{40}H_{46}N_8O_{10}Ni_2Cu$)

Element analysis: Expected % C: 49.04, H: 4.73, N: 11.43, % Ni: 11.98, % Cu: % 6.49; Found % C: 48.76, H: 4.36, N: 10.95, Ni: 11.29, Cu: 6.31.

Important IR data (cm^{-1}): $\nu_{C-H(Ar)}$: 3048–3029, $\nu_{C-H(Aliph)}$: 2924–2873, $\nu_{C=O(DMF)}$: 1658, $\nu_{C=N}$: 1627, $\nu_{C=C(ring)}$: 1596, $\nu_{N=O}$: 1309, δ_{CH2}: 1473, $\nu_{C-O(Phenol)}$: 1197–1153, $\delta_{C-H(Ar)}$: 759.

Complex II, {[DMF·NiL·Cu(NO$_3$)$_2$·NiL·DMF]·DMF} ($C_{43}H_{53}N_9O_{13}Ni_2Cu$)

Element analysis: Expected % C: 47.61, H: 4.92, N: 11.61, % Ni: 10.82, % Cu: % 5.85; Found % C: 47.11, H: 4.59, N: 10.33, Ni: 10.23, Cu: 6.07 (This molecule is included 1 molecule DMF as solvate).

Important IR data (cm^{-1}): $\nu_{C-H(Ar)}$: 3038–3026, $\nu_{C-H(Aliph)}$: 2922–2845, $\nu_{C=O(DMF)}$: 1670, $\nu_{C=N}$: 1631, $\nu_{C=C(ring)}$: 1595, $\nu_{N=O}$:1417–1440, δ_{CH2}: 1473, $\nu_{C-O(Phenol)}$: 1296–1253, $\delta_{C-H(Ar)}$: 756.

Complex III, [DMF·NiL·Ni(NO$_2$)$_2$·NiL·DMF] ($C_{40}H_{46}N_8O_{10}Ni_3$)

Element analysis: Expected % C: 49.28, H: 4.76, N: 11.49, % Ni: 18.06; Found % C: 48.51, H: 4.43, N: 10.85, Ni: 17.44.

Important IR data (cm^{-1}): $\nu_{C-H(Ar)}$: 3040–3023, $\nu_{C-H(Aliph)}$: 2924–2839, $\nu_{C=O(DMF)}$: 1672, $\nu_{C=N}$: 1628, $\nu_{C=C(ring)}$: 1595, $\nu_{N=O}$: 1309, δ_{CH2}: 1473, $\nu_{C-O(Phenol)}$: 1195, $\delta_{C-H(Ar)}$: 758.

Complex IV, {[DMF·NiL·Ni(NO$_3$)$_2$·NiL·DMF](DMF)$_2$} ($C_{46}H_{60}N_{10}O_{12}Ni_3$)

Elemental analysis: Expected % C: 49.28, H: 5.39, N: 12.48, % Ni: 15.70; Found % C: 48.69, H: 4.91, N: 11.87, Ni: 151.22, Cu: 6.31 (This molecule is included 2 molecules DMF as solvate).

Important IR data (cm^{-1}): $\nu_{C-H(Ar)}$: 3044–3027, $\nu_{C-H(Aliph)}$: 2922–2862, $\nu_{C=O(DMF)}$: 1671, $\nu_{C=N}$: 1629, $\nu_{C=C(ring)}$: 1595, $\nu_{N=O}$: 1400, δ_{CH2}: 1473, $\nu_{C-O(Phenol)}$: 1193–1074, $\delta_{C-H(Ar)}$: 754.

Preparation of the complex V

This complex was prepared by template method. A quantity of 0.002 mol (0.640 g) bis-*N*,*N*′(2-hydroxyacetophenilidene)-1,3-propanediamine was dissolved in 40 mL DMF by heating. To this solution was added 1.0 mL Et_3N and a solution of 0.002 mol (0.472 g) $NiCl_2{\cdot}6H_2O$ in 20 mL hot MeOH then finally was added to the mixture a solution of 0.001 mol (2.41 g) $Cu(NO_3)_2{\cdot}3H_2O$ in 10 mL hot MeOH. The resulting mixture was set aside for 4 days, and the precipitated crystals were filtered and dried in air.

Scheme 2 Preparing trinuclear complex with Schiff bases and mononuclear complexes

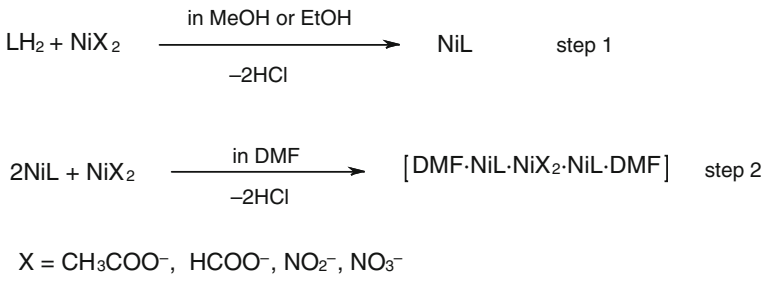

{[DMF·NiLAC·Cu(NO$_3$)$_2$·NiLAC·DMF](DMF)}, ($C_{47}H_{61}N_9O_{13}Ni_2Cu$)

Elemental analysis: Expected % C: 49.49, H: 5.39, N: 11.05, % Ni: 10.27, Cu: 5.57; Found % C: 47.98, H: 4.75, N: 10.63, Ni: 9.62, Cu: 5.74.

Important IR data (cm^{-1}): $\nu_{C-H(Ar)}$: 3055–3020, $\nu_{C-H(Aliph)}$: 2931–2839, $\nu_{C=O(DMF)}$: 1672, $\nu_{C=N}$:1630, $\nu_{C=C(ring)}$: 1595, $\nu_{N=O}$: 1438–1328, δ_{CH2}: 1473, $\nu_{C-O(Phenol)}$: 1244–1134, $\delta_{C-H(Ar)}$: 750.

Preparation of the complexes with reduced Schiff base, complex VI–IX

These complexes were synthesized by template method according to the Scheme 1 and the literature [18, 24, 26, 44]. A quantity of 0.002 mol (0.572 g) the reduced Schiff base bis-*N*,*N*′(2-hydroxybenzyl)-1,3-propanediamine was dissolved in 40 mL DMF under heating and mixed. 1.0 mL Et_3N and a solution of 0.002 mol (0.472 g) $NiCl_2{\cdot}6H_2O$ in 20 mL hot MeOH were added to this solution. Then, for complex VI 0.001 mol (0.170 g) $CuCl_2{\cdot}2H_2O$ and 0.002 mol (0.140 g) $NaNO_2$, for complex VII 0.001 mol (2.41 g) $Cu(NO_3)_2{\cdot}3H_2O$, for complex VIII 0.001 mol (0.236 g) $NiCl_2{\cdot}2H_2O$ and 0.002 mol (0.140 g) $NaNO_2$ and for complex IX 0.001 mol (0.291 g) $Ni(NO_3)_2{\cdot}6H_2O$ were dissolved in 30 mL water–MeOH mixture (v/v: %50–%50) using heating and mixed with the above mixture. The resulting mixture was set aside for 4–5 days, and after this period, the crystal products were filtered and dried in air. The analytical results of these complexes are given below.

Complex VI, [DMF·NiL^H·Cu(NO$_2$)$_2$·NiL^H·DMF], ($C_{40}H_{54}N_8O_{10}Ni_2Cu$)

Elemental analysis: Expected % C: 48.64, H: 5.51, N: 11.34, % Ni: 11.85, Cu: 6.43; Found % C: 47.99, H: 5.08, N: 10.97, Ni: 11.41, Cu: 5.96.

Important IR data (cm^{-1}): ν_{N-H}: 3169–3143, $\nu_{C-H(Ar)}$: 3041–3021, $\nu_{C-H(Aliph)}$: 2924–2858, $\nu_{C=O(DMF)}$: 1659, $\nu_{C=C(ring)}$:1595, $\nu_{N=O}$:1425, δ_{CH2}: 1483, $\nu_{C-O(Phenol)}$: 1284–1259, $\delta_{C-H(Ar)}$: 748.

Complex VII, [DMF·NiL^H·Cu(NO$_3$)$_2$·NiL^H·DMF], ($C_{40}H_{54}N_8O_{12}Ni_2Cu$)

Elemental analysis: Expected % C: 47.12, H: 5.34, N: 10.98, Ni: 11.48, Cu: 6.27; Found % C: 46.59, H: 5.13, N: 10.66, Ni: 11.07, Cu: 6.92.

Important IR data (cm^{-1}): ν_{N-H}: 3167–3140, $\nu_{C-H(Ar)}$: 3043–3021, $\nu_{C-H(Aliph)}$: 2918–2868, $\nu_{C=O(DMF)}$: 1658, $\nu_{C=C(ring)}$: 1598, $\nu_{N=O}$: 1425–1396, δ_{CH2}: 1483, $\nu_{C-O(Phenol)}$: 1274–1257, $\delta_{C-H(Ar)}$: 750.

Complex VIII, [DMF·NiL^H·Ni(NO$_2$)$_2$·NiL^H·DMF], ($C_{40}H_{54}N_8O_{10}Ni_3$)

Elemental analysis: Expected % C: 48.89, H: 5.54, N: 11.34, Ni: 11.39; Found % C: 48.53, H: 4.98, N: 11.18, Ni: 10.34.

Important IR data (cm^{-1}): ν_{N-H}: 3186–3144, $\nu_{C-H(Ar)}$: 3047–3033, $\nu_{C-H(Aliph)}$: 2938–2861, $\nu_{C=O(DMF)}$: 1655, $\nu_{C=C(ring)}$: 1593, $\nu_{N=O}$: 1413–1384, δ_{CH2}: 1481, $\nu_{C-O(Phenol)}$: 1312–1280, $\delta_{C-H(Ar)}$: 756.

Complex XI, [DMF·NiL^H·Cu(NO$_3$)$_2$·NiL^H·DMF], ($C_{40}H_{54}N_8O_{12}Ni_3$)

Elemental analysis: Expected % C: 47.35, H: 5.36, N: 11.04, Ni: 17.35; Found % C: 46.87, H: 4.88, N: 10.57, Ni: 16.09.

Important IR data (cm^{-1}): ν_{N-H}: 3246, $\nu_{C-H(Ar)}$: 3036–3017, $\nu_{C-H(Aliph)}$: 2922–2858, $\nu_{C=O(DMF)}$: 1652, $\nu_{C=C(ring)}$: 1593, $\nu_{N=O}$: 1419–1385, δ_{CH2}: 1481, $\nu_{C-O(Phenol)}$: 1313–1275, $\delta_{C-H(Ar)}$: 756.

Results and discussion

As mentioned in introduction part, complexes including nitrite and nitrate ions were reported in the literature as μ-bridge [15–18, 20]. Molecular models were determined by X-ray diffraction in literature studies. Nitrate ion links Ni (II) ions and central metal ions with two oxygen, while

nitrite ion is linked to terminal Ni(II) ions with one oxygen links to central metal ion via nitrogen atom. As mentioned above, complex V was synthesized by using a different Schiff base. Purpose of preparing this complex is to show the condition of nitrate bridge once again in parallel to the literature. For complex V, pluton drawing obtained by X-ray diffraction works is given in Fig. 9. Crystallographic data and experimental data of complex V, and important angles and lengths around coordination sphere are given in Tables 1 and 2, respectively.

As shown in Fig. 9, terminal ion Ni(II) exists between two phenolic oxygen, two iminic nitrogen and one DMF molecule oxygen and one nitrate oxygen O_4N_2 donor atoms, while central Cu(II) ion exists among four phenolic oxygen and two nitrate oxygen in O_6 coordination sphere. As it can be seen, there are two different μ-bridges as phonologic oxygen and nitrates-constituted μ-bridges. Complexes prepared by LH_2 vs L^HH_2 are in similar structure. Complexes I–V and other complex groups VI–IX were examined by TG, and significant differences were observed between TG curves. In Fig. 10, TG curves of I–IV-numbered complexes are seen in a body, and DTA curves of these materials are shown in Fig. 11 together. TG curves of VI–IX-numbered complexes are shown in Fig. 12, and DTA curves of these complexes are shown in Fig. 13.

As shown in Figs. 10 and 12, TG curves of both groups are different from each other. In complexes prepared by Schiff bases, two thermal reactions are observed, and the ones contained in DMF as solvate, three thermal reactions are observed. On the other hand, complexes prepared by reduced Schiff bases, only one thermal reaction was observed. The first mass loss seen on the curves depicted in red and green colors corresponds to one- and two-molecule DMF existing as solvate. Second mass losses in Fig. 10 are not clearly seen in the nitrite including complexes; however, it can be stated that these mass losses correspond to two coordinative DMF existing in trinuclear complex. Similar case can be seen on DTA curves. First endothermic reactions observed in Fig. 11 belong to DMF molecules existing as solvate, second endothermic signals belong to separation of coordinative DMF molecules and last two signals belongs to three thermal reactions of nitrite and nitrate containing complexes. However, in Fig. 13, it is seen that one thermal reaction is exothermic in four complexes prepared with reduced Schiff base. Thermoanalytical data obtained from these curves are given in Table 3.

As shown in Figs. 10, 11 and Table 3 in Schiff base complexes, the ones containing nitrite, DMF molecules are separated from structure at 180–200 °C. In this case, there is only NiL, and nitrite or nitrate salts are remained in the environment. It is known that mixture of nitrite and nitrate ions in organic material behaves as energetic material in higher temperatures [45]. In this case, residual nitrite or nitrate rapidly oxidizes a part of NiL mononuclear complex

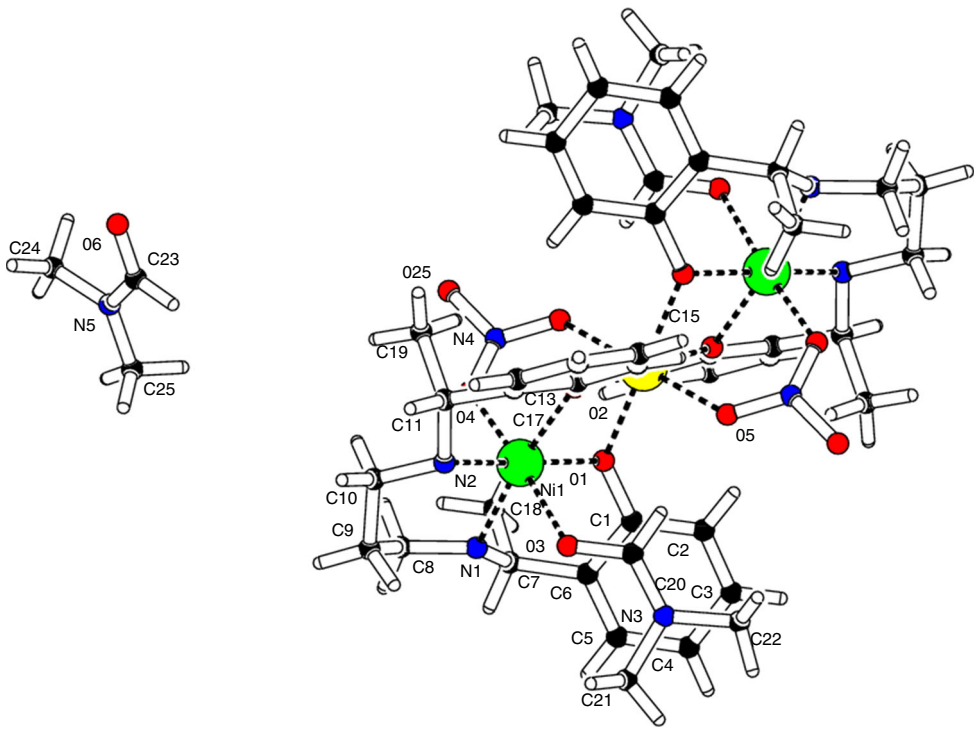

Fig. 9 {[DMF·NiLAC·Cu$(NO_3)_2$·NiLAC·DMF]·DMF} pluton drawing of complex V. One molecule exists as DMF solvate in crystal structure

Table 1 Crystallographic and experimental data of complex V

Formula weight/g mol^{-1}	$C_{47}H_{61}N_9O_{13}Ni_2Cu$
T/K	100 (2)
Crystal size/mm	0.64 × 0.42 × 0.14
Crystal system	Monoclinic
Space group	$P2_1/c$
a/Å	11.9957 (6)
b/Å	15.2470 (7)
c/Å	15.5784 (9)
Alpha	90.00
Beta	96.615 (7)
Gamma	90.00
V/$Å^3$	2830.3 (3)
Z	2
Calc. density/g cm^{-3}	1.425
μ/mm^{-1}	1.102
F (000)	1270
T_{min}–T_{max}	0.5391–0.8611
θ Range/°	2.95–28.24
Index ranges	$-14 \le h \le 13$, $-18 \le k \le 19$, $-19 \le l \le 19$
Reflections collected	5949
Reflections unique	4249
*R*1, w*R*2 (2ó)	0.1092, 0.3248
*R*1, w*R*2 (all)	0.1313, 0.3448
Data/parameters	5949/379
GOOF of F^2	1.341
Largest difference peak hole/ e $Å^{-3}$	−1.337, 3.410
CCDC No	1,481,757

Table 2 Selected bond length and angle values around of coordination sphere

Bond length/Å	Bond angles/°
N1 Ni1 2.087(5)	O4 Ni1 O2 91.69(18)
N2 Ni1 2.095(5)	O4 Ni1 O1 90.47(17)
N4 O4 1.251(8)	O2 Ni1 O1 82.94(16)
N4 O5 1.273(7)	O4 Ni1 N1 93.6(2)
N4 O25 1.505(10)	O2 Ni1 N1 172.48(18)
O1 Ni1 2.039(4)	O1 Ni1 N1 91.63(18)
O1 Cu1 2.069(4)	O4 Ni1 N2 94.3(2)
O2 Ni1 2.030(4)	O2 Ni1 N2 90.68(19)
O2 Cu1 2.052(4)	O1 Ni1 N2 172.1(2)
O3 Ni1 2.192(5)	N1 Ni1 N2 94.3(2)
O4 Ni1 2.016(4)	O4 Ni1 O3 175.44(17)
O5 N4 1.273(7) 3	O2 Ni1 O3 92.55(18)
O5 Cu1 2.095(4)	O1 Ni1 O3 91.71(17)
Cu1 O2 2.052(4)	N1 Ni1 O3 82.4(2)
Cu1 O1 2.069(4)	N2 Ni1 O3 84.0(2)
Cu1 O5 2.095(4)	O2 Cu1 O2 180.0(2)
	O2 Cu1 O1 81.67(16)
	O2 Cu1 O1 98.33(16)
	O2 Cu1 O1 98.33(16)
	O2 Cu1 O1 81.67(16)
	O1 Cu1 O1 180.0(2)
	O2 Cu1 O5 93.21(17)
	O2 Cu1 O5 86.79(17)
	O1 Cu1 O5 93.91(16)
	O1 Cu1 O5 86.09(16)
	O2 Cu1 O5 86.79(17)
	O2 Cu1 O5 93.21(17)
	O1 Cu1 O5 86.09(16)
	O1 Cu1 O5 93.91(16)
	O5 Cu1 O5 180.0(3)

and a reaction similar to explosion reaction is observed. This explosion reaction is observed in nitrate complexes (complex II and IV) around 330 °C and is observed around 280 °C in nitrite complexes (complex I and III). This situation arises due to possible nitrate and nitrite is coordinated from different atoms. While complexes with nitrite are coordinated on oxygen and nitrogen, nitrate complexes are coordinated on two oxygen atoms. Same situation is seen on reduced Schiff base complexes. Complexes including nitrite (complex VI and VIII) give explosion reaction around 230 °C, and complexes including nitrate give explosion reaction around 260 °C. Mass loss observed in reduced complexes is a little bit higher than Schiff base complexes. Above-mentioned thermoanalytical data indicate that mononuclear NiL^H complex is stable at some reduced Schiff base complexes. One NiL^H complex could not be prepared between L^HH_2 and Ni (II) ion. In spite of this when L^HH_2 was used, trinuclear complex was easily prepared by template method. This situation shows L^HH_2 ligand complexes are stable at trinuclear state. TG results support this suggestion. In complexes prepared by Schiff bases, DMF molecules are separated from structure in a certain temperature range around 150–160 °C suggesting that trinuclear complex is decomposed probably, and here, the residual is NiL and nitrate salt. NiL could be prepared as mononuclear complex and could be obtained as stable form. In reduced Schiff bases because NiL^H is not stable structure, trinuclear complex can stand up to 250 °C and decompose in this temperature with explosion reaction, in this situation mass loss is a little bit higher comparing to Schiff base complexes. Due to NiL^H is an unstable mononuclear complex, trinuclear complex should be more tensed and unstable compared to Schiff base complexes. Thermokinetic calculations were done with this consideration. Thermokinetic calculations were performed according to Ozawa [29, 30], Ozawa–Flynn–Wall (OFW) [31–35] and Kissenger–Akahira–Sunose (KAS) [33–37]

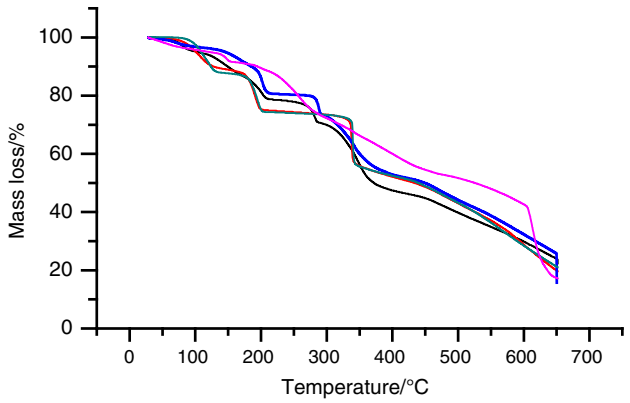

Fig. 10 TG curves of complexes I–V. *Black* [DMF·NiL·Cu$(NO_2)_2$·NiL·DMF] (I), *Red* {[DMF·NiL·Cu$(NO_3)_2$·NiL·DMF]DMF} (II), *Blue* [DMF·NiL·Ni$(NO_2)_2$·NiL·DMF] (III), *Green* {[DMF·NiL·Ni$(NO_3)_2$·NiL·DMF]2DMF} (IV), *Pink* [DMF·NiLAC·Cu$(NO_3)_2$·NiLAC·DMF]. (Color figure online)

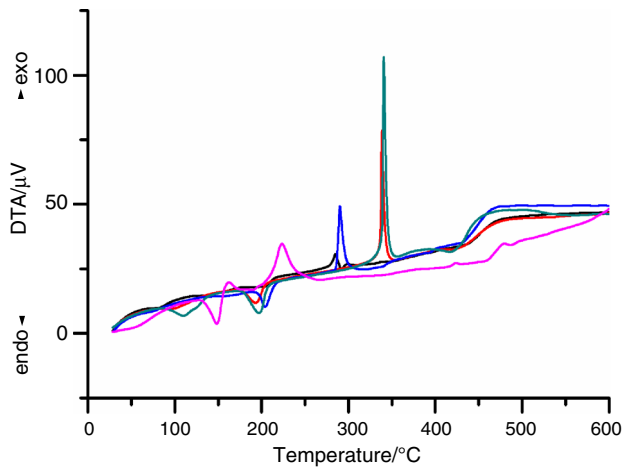

Fig. 11 DTA curves of complexes I–V. *Black* [DMF·NiL·Cu$(NO_2)_2$·NiL·DMF] (I), *Red* {[DMF·NiL·Cu$(NO_3)_2$·NiL·DMF]DMF} (II), *Blue* [DMF·NiL·Ni$(NO_2)_2$·NiL·DMF] (III), *Green* {[DMF·NiL·Ni$(NO_3)_2$·NiL·DMF]2DMF} (IV), *Pink* {[DMF·NiLAC·Cu$(NO_3)_2$·NiLAC·DMF]DMF}. (Color figure online)

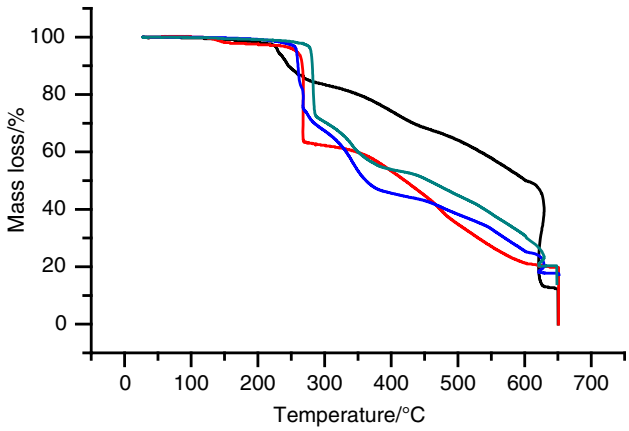

Fig. 12 TG curves of complexes VI–IX. *Black* [DMF·NiL^H·Cu$(NO_2)_2$·NiL^H·DMF] (VI), *Red* [DMF·NiL^H·Cu$(NO_3)_2$·NiL^H·DMF] (VII), *Blue* [DMF·NiL^H·Ni$(NO_2)_2$·NiL^H·DMF] (VIII), *Green* [DMF·NiL^H·Ni$(NO_3)_2$·NiL^H·DMF] (IX). (Color figure online)

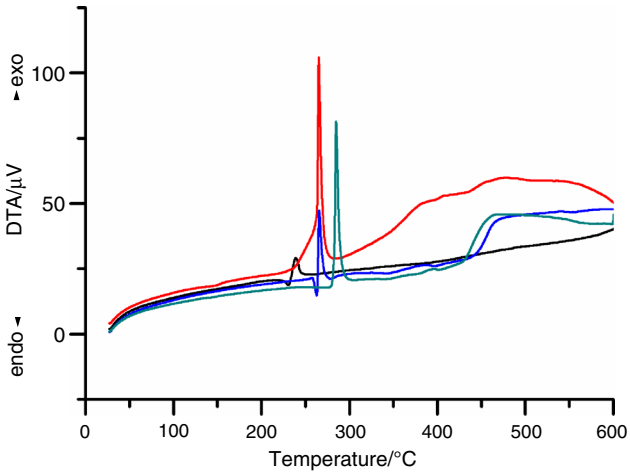

Fig. 13 DTA curves of complexes VI–IX. *Black* [DMF·NiL^H·Cu$(NO_2)_2$·NiL^H·DMF] (VI), *Red* [DMF·NiL^H·Cu$(NO_3)_2$·NiL^H·DMF] (VII), *Blue* [DMF·NiL^H·Ni$(NO_2)_2$·NiL^H·DMF] (VIII), *Green* [DMF·NiL^H·Ni$(NO_3)_2$·NiL^H·DMF] (IX). (Color figure online)

equations; isothermal calculations were done according to Coats–Redfern (CR) equations from non-isothermal methods. Equations used in these calculations are given as follows:

Ozawa:

$$\log \beta = \log\left[\frac{AE_a}{Rg(\alpha)}\right] - 2.315 - 0.4567\left[\frac{E_a}{RT}\right]$$

OFW:

$$\mathrm{In}\beta = \mathrm{In}\left[\frac{0.0048AE_a}{Rg(\alpha)}\right] - 1.0516\left[\frac{E_a}{RT}\right]$$

KAS:

$$\mathrm{In}\left[\frac{\beta}{T^2}\right] = \mathrm{In}\left[\frac{AE_a}{Rg(\alpha)}\right] - \left[\frac{E_a}{RT}\right]$$

Coats–Redfern:

$$\mathrm{In}\left[\frac{g(\alpha)}{T^2}\right] = \mathrm{In}\left[\frac{AR}{\beta E_a}\right] - \left[\frac{E_a}{RT}\right]$$

where β is a heating speed as °C min^{-1}, R universal gas constant, E_a thermal disintegration activation energy, A Arrhenius pre-exponential factor, T temperature in K, $g(\alpha)$ fractional completed fraction of thermal fracture reaction.

Table 3 Thermoanalytical data of the complex I–IX

Complexes	First thermal reaction solvate DMF mass loss endothermic		Second thermal reaction coordinative DMF mass loss, endothermic		Third thermal reaction mass loss of detonation, exothermic	
	Temperature range/°C	Mass loss % Exp./% found	Temperature range	Mass loss % Exp./% found	Temperature range/°C	Mass loss % found
[DMF·NiL·Cu $(NO_2)_2$·DMF]·1/2DMF complex I	55–92/DTA peak:74	4.52/4.58 ± 0.08	176–211/DTA peak:199	14.37/9.07 ± 0.07	256–291/DTA peak:274	8.06 ± 0.83
[DMF·NiL·Cu $(NO_3)_2$·DMF]·DMF complex II	66–112/DTA peak:90	6.73/10.30 ± 0.16	161–193/DTA peak:188	13.47/13.45 ± 0.17	325–342/DTA peak:333	21.38 ± 3.26
[DMF·NiL·Ni $(NO_2)_2$·DMF]·complex III			180–206/DTA peak:200	14.98/14.04 ± 1.02	273–295/DTA peak:283	9.37 ± 1.03
{[DMFNiL·Ni$(NO_3)_2$·NiL·DMF]2DMF} complex IV	73–122/DTA peak:98	12./12.40 ± 0.28	168–202/DTA peak:185	12.97/12.81 ± 0.12	325–342/DTA peak:332	19.73 ± 2.78
{[DMF·NiLAC·Cu$(NO_3)_2$·NiLAC·DMF]DMF} complex V	48–97/DTA peak:70.08	6.40/5.84 ± 0.95	125–179/DTA peak:145	12.81/10.97 ± 1.29	185–247/DTA peak:185	14.48 ± 0.91
[DMF·NiL^H·Cu$(NO_2)_2$·NiL^H·DMF] complex VI					222–254/DTA peak:229	13.39 ± 1.89
[DMF·NiL^H·Cu$(NO_3)_2$·NiL^H·DMF] complex VII					233–267/DTA peak:242	27.97 ± 0.79
[DMF·NiL^H·Ni$(NO_2)_2$·NiL^H·DMF] complex VIII					222–269/DTA peak:264	34.23 ± 2.48
[DMF·NiL^H·Ni$(NO_3)_2$·NiL^H·DMF] complex IX					267–288/DTA peak:279	30.70 ± 0.22

These equations were generated considering reaction order $n = 1$ and realized as mentioned above.

$$A_{solid} \rightarrow B_{solid} + C_{gas}$$

For Coats–Redfern equation, $\beta = 10$ °C min^{-1} and $g(\alpha)$ value were calculated between 0.1 and 0.9 and calculations were made by graphic assistance. In application of non-isothermal methods, β value changed in the range of 5, 10, 15, 20, 25 °C min^{-1} and graphical results were obtained. On software of TG device, there is extra software for Ozawa method; for that reason, Ozawa results were calculated from software of device (TA Workstation, TA60 kinetic analysis Program, version 2.01, Shimadzu Corp.). But software gave error signal for nitrite and nitrate ion explosions.

FOW and KAS methods were performed by manipulation. But since temperature change showed anomaly for explosion reactions of nitrite and nitrate ions, $g(a)$ calculation was able to be done by taking the values between 0.05–0.18 and 0.85–0.95. Results calculated according to four methods are given in Tables 6 and 7. As shown in Fig. 10 and Table 3 for complexes prepared from Schiff bases (I–IV), there are two thermal reactions: First reaction is the separation of coordinative DMF molecules and second reaction is the explosion reaction of nitrite and nitrate. These values were calculated for both reactions. From the above equation, E_a and A values could be calculated. Thermodynamic parameters in thermal reaction could be calculated by using these values.

$$\Delta S = 2.303\left[\log\frac{Ah}{kT}\right]R$$

$$\Delta H = E_a - RT$$

$$\Delta G = \Delta H - T\Delta S$$

Separation of coordinative DMF molecules reaction only exists for I–IV-numbered complexes as it is shown in Fig. 10 as well. The results found by the above equations for the DMF thermal separation reaction are given in Table 4. According to the method, E_a and A values were calculated different for this DMF separation reaction. By the way, three Arrhenius pre-exponential constant value (A) is significantly different compared to others; A value calculated with OFW method for complex I, A value calculated with KAS method for complex II and A value calculated with CR equation for complex IV are also found significantly different; other values are in comparable sizes.

As shown in Table 4, Ozawa software gave no results for complex II, IV and VII. Only two of results, complex I and Complex VI (respectively, 123 and 113.35 kJ mol^{-1}, $1.76.10^{11}$ min^{-1}), obtained from Coast–Redfern equation could be comparable with other results for E_a and A values. Other values calculated by Coats–Redfern equation are

Table 4 Thermokinetic results of complex I–IV for DMF removal reaction (first thermal reaction)

Complex	Methods							
	Ozawa		Coats–Redfern		OFW		KAS	
	E_a/kJ mol^{-1}	Arrhenius pre-exponential factor/min^{-1}	E_a/kJ mol^{-1})/R^2 (regression value)	Arrhenius pre-exponential factor/min^{-1}	E_a/kJ mol^{-1})/R^2 (regression value)	Arrhenius pre-exponential factor/min^{-1}	E_a/kJ mol^{-1})/R^2 (regression value)	Arrhenius pre-exponential factor/min^{-1}
I	159.36 ± 4.12	1.40×10^{12}	134.03 ± 3.49/0.9864	2.56×10^{14}	258.89 ± 9.22/0.9495	3.43×10^{19}	249.92 ± 8.84/0.9430	1.48×10^{18}
II	106.53 ± 7.50	8.71×10^{10}	167.79 ± 7.64/0.9182	2.11×10^{12}	83.63 ± 0.30/0.9960	1.49×10^{9}	81.19 ± 0.29/0.9958	4.65
III	169.27 ± 14.10	2.72×10^{12}	141.49 ± 8.05/0.8408	2.91×10^{15}	117.28 ± 2.43/0.9493	2.81×10^{12}	115.73 ± 2.34/0.9451	8.93×10^{3}
IV	113.51 ± 5.02	2.33×10^{8}	177.83 ± 3.80/0.9480	1.09×10^{20}	83.12 ± 0.79/0.9723	2.36×10^{9}	75.16 ± 0.76/0.9642	1.31×10^{9}

significantly higher; E_a and A values were calculated higher, and as a result, other thermodynamic parameters are calculated different. In explosion reaction of nitrate and nitrite ions, Ozawa method and OFW methods gave quite similar results. Only if E_a values are compared, OFW and Ozawa obtained from KAS method is similar, but A value calculated with KAS is as small as not comparable.

Values specified in Table 5 are the rates which were calculated for explosion reaction of nitrite and nitrate ions with an organic substance. Ozawa software did not give any result for three complexes. These are complexes containing nitrate. As it is known nitrate and nitrite ions are oxidizing ions, they oxidize organic substance with organic substance rapidly and cause rapid explosive reaction. First explosive substance black powder contains nitrate salt, coal dust and elemental dust sulfur in [45]. Nitrate includes more oxygen atom, and for that reason, mass loss and liberated energy in nitrated complexes are more in explosion reaction and this situation is shown in Figs. 10, 11 and Table 3. Gas product amount is expected to be excessive in nitrate complex explosion reactions, since it is a rapid reaction during the diffusion of these gas products, temperature distribution around pan is contrary to expectation. Temperature increases in a short time during explosion. But gas product amount is high, and during the diffusion of gas molecules around pan, temperature is decreased again which is a result of heat transfer of these gas molecules. This situation creates an anomaly in TG curve. Figure 14 shows TG curve of {[DMF·NiL·Ni$(NO_3)_2$·NiL·DMF]·2DMF}, complex IV, and Fig. 15 shows DTA curve in detail. Here, there can be seen three reactions, first reaction is a mass loss belonging to DMF's which exist as solvate separation; it has been occured between 73 and 122 °C. Second thermal reaction belongs to coordinative DMF's loss and occured between 168 and 202 °C. Third thermal reaction is explosion reaction. This explosion reaction was occured between 325 and 342 °C. Mass loss at the beginning of explosion reaction shows a negative slope as expected. But as long as the reaction forwards, slope goes through positive side because temperature does not increase but decreases in contrary, because the gases generated during the explosion and move away quickly and this generated gases carry out the reaction heat from Pt pan. For this reason, the temperature decreases during explosion reaction. In DTA curve, extraordinary cycle is observed instead a Gaussian-type signal. This situation is clearly shown in Figs. 14 and 15. Two thermal reactions were proceeded as expected. The mass loss increased with temperature increases and expected TG curves were calculated, but it is seen that mass loss and temperature decreased in third thermal reaction. In parallel to this, signals of first two thermal reactions are normal endothermic signals in Fig. 15, but there is an anomaly in

Table 5 Thermokinetic results of complex I–IV, VI–IX for explosion reaction of nitrite or nitrate ions (second thermal reaction)

Complexes	Methods							
	Ozawa		Coats–Redfern		OFW		KAS	
	E_a/kJ mol^{-1}	Arrhenius pre-exponential factor/ min^{-1}	E_a/kJ mol^{-1})/R^2 (regression value)	Arrhenius pre-exponential factor/ min^{-1}	E_a/kJ mol^{-1}	Arrhenius pre-exponential factor/ min^{-1}	E_a/kJ mol^{-1})/R^2 (regression value)	Arrhenius pre-exponential factor/ min^{-1}
I	137.62 ± 12.99	5.92×10^{11}	123.49 ± 3.45/0.9740	2.36×10^{11}	135.95 ± 5.16/0.969	9.39×10^{13}	128.82 ± 2.32/0.963	244.41
II	Could not calc.		484.37 ± 23.78/0.9867	4.14×10^{41}	158.52 ± 3.08/0.983	2.67×10^{11}	165.22 ± 3.04/0.9814	4.28×10^{5}
III	131.56 ± 1.47	8.27×10^{8}	284.35 ± 13.64/0.9864	2.43×10^{26}	142.78 ± 3.79/0.9379	7.97×10^{11}	138.88 ± 4.79/0.9977	21.34
IV	Could not calc.		232.83 ± 9.37/0.9881	1.38×10^{19}	111.47 ± 1.13/0.9890	1.53×10^{9}	107.83 ± 1.09/0.9872	2.87
VI	129.59 ± 4.51	1.02×10^{15}	113.35 ± 0.84/0.9390	1.76×10^{11}	118.45 ± 1.87/0.9743	2.47×10^{14}	115.56 ± 1.98/0.9690	6194.76
VII	Could not calc.		515.44 ± 9.28/0.9776	1.76×10^{45}	125.31 ± 1.97/0.9703	5.02×10^{10}	122.88 ± 1.96/0.9656	1177.53
VIII	124.28 ± 8.18	1.84×10^{9}	369.54 ± 10.72/0.8948	1.38×10^{36}	125.36 ± 1.12/0.9887	1.55×10^{11}	116.29 ± 1.34/0.9867	338.32
IX	Could not calc.		519.84 ± 11.44/0.9729	1.27×10^{50}	131.47 ± 4.53/0.9389	5.50×10^{12}	128.86 ± 4.09/0.9211	1125.17

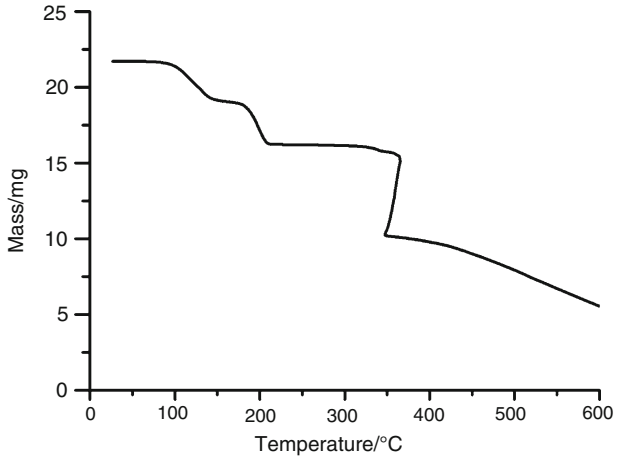

Fig. 14 TG curve of the complex IV ({[DMF·NiL·Ni(NO$_3$)$_2$·NiL·DMF]·2DMF})

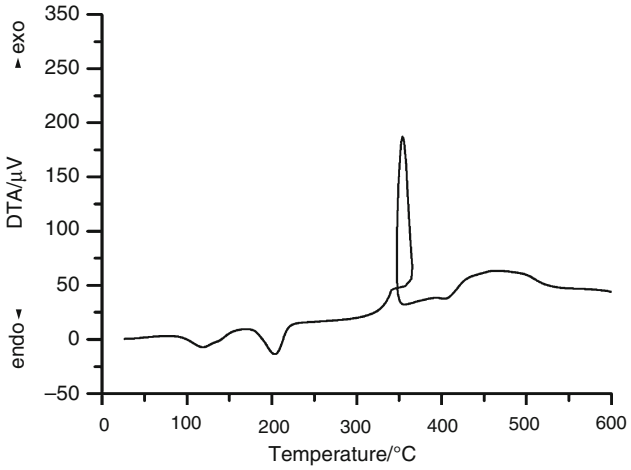

Fig. 15 DTA curve of the complex IV ({[DMF·NiL·Ni(NO$_3$)$_2$·NiL·DMF]·2DMF})

third thermal reaction signal. In this situation, according to Ozawa, OFW or KAS method, graphics drawn between $g(\alpha)$'s proper values (0.2–0.8), the lines deviate from linearity. For that reason, Ozawa software is failed. In spite of this in graphics which were drawn according to another methods, $g(\alpha)$ values were calculated by taking relatively closer to limit values.

Our general remarks were summarized in results given in Tables 4 and 5

1. As mentioned before, coordinative DMF loss was occurred as expected manner and observed as endothermic reaction. Results which were found according to four different methods for this thermal reaction are comparable values to each other. There are differences between the results calculated by these methods, but this is a common situation for these semi-experimental methods in the literature [32, 35]. Only

Table 6 Calculated thermodynamic parameters for DMF removal reaction (first thermal reaction)

Complex	Methods											
	Ozawa			Coats–Redfern			OFW			KAS		
	ΔH/ kJ mol^{-1}	ΔS/ J K^{-1}	ΔG/ kJ mol^{-1}	ΔH/ kJ mol^{-1}	ΔS/ J K^{-1}	ΔG/ kJ mol^{-1}	ΔH^*/ kJ mol^{-1}	ΔS/ J K^{-1}	ΔG/ kJ mol^{-1}	ΔH/ kJ mol^{-1}	ΔS/ J K^{-1}	ΔG/ kJ mol^{-1}
I	155.26	−16.57	163.93	130.01	26.90	116.75	254.79	266.67	123.32	245.82	98.78	197.12
II	101.35	−41.60	127.67	163.44	99.04	101.74	78.45	−75.43	125.44	76.01	−238.29	224.46
III	169.92	−11.53	175.95	137.14	46.47	112.84	112.93	−11.26	118.82	113.38	−173.97	204.36
IV	109.16	−89.41	155.92	151.71	134.04	85.60	78.66	−70.16	115.35	111.00	−75.05	150.25

Table 7 Calculated thermodynamic parameters for explosion reactions of nitrite or nitrate ions (second thermal reaction)

Complex	Methods											
	Ozawa			Coats–Redfern			OFW			KAS		
	ΔH/ kJ mol^{-1}	ΔS/ J K^{-1}	ΔG/ kJ mol^{-1}	ΔH/ kJ mol^{-1}	ΔH/ kJ mol^{-1}	ΔS/ J K^{-1}	ΔG/ kJ mol^{-1}	ΔH/ kJ mol^{-1}	ΔH/ kJ mol^{-1}	ΔS/ J K^{-1}	ΔG/ kJ mol^{-1}	ΔH/ kJ mol^{-1}
I	137.62	−25.26	152.59	118.56	−32.90	138.07	131.89	18.47	122.86	114.75	−203.33	214.18
II				478.44	546.18	154.55	154.50	−30.17	169.07	161.20	−141.13	240.66
III	126.63	−79.92	173.42	279.42	254.54	128.47	138.66	−21.28	149.19	104.76	−223.71	215.49
IV				228.15	115.81	159.47	107.44	−73.11	142.82	103.81	−240.21	220.07
VI	124.91	37.13	104.00	108.67	−34.91	129.37	114.03	28.82	98.69	111.14	−177.16	205.39
VII				510.67	615.66	145.58	120.63	−44.17	145.49	118.19	−191.43	225.96
VIII	119.52	−72.98	161.33	364.77	441.31	103.07	120.58	−36.14	141.61	111.45	−202.08	229.06
IX	141.12	1.89	139.99	514.91	708.68	94.66	126.64	−6.54	130.78	123.61	−192.77	243.44

Arrhenius pre-exponential factor values that were calculated by KAS method are different from others. Due to loss of DMF was observed on Schiff base complexes (complexes I–IV), it is not possible to compare these results with reduced Schiff base results.

2. Explosion reaction caused by nitrate and nitrite ions was seen at all eight complexes too. As mentioned before, due to explosion is severe in complexes containing nitrate and TG curves showed anomaly, calculations were performed only at higher $g(\alpha)$ values. As shown in Table 5 according to Coats–Redfern equation, calculated values are higher than others, Arrhenius pre-exponential constant values are at unacceptable sizes. Ozawa and OFW results are overlapped; in E_a, results obtained by KAS method are comparable sizes with these values, but Arrhenius pre-exponential constant values that were calculated by KAS are not acceptable again. Purpose of this study was to determine the strains of two different species by comparison. Because while NiL has been able to synthesized and isolated, it was not possible to isolate NiL^H and still trinuclear complexes of both mononuclear complexes have been able to prepare. If NiL^H had a strain, this instability should have been in trinuclear complexes. In this situation, E_a value which was calculated by thermokinetic methods is expected to be lower. Study was carried out in order to support this suggestion. But due to explosion reactions did not give expected TG curve, robust comparison results were not calculated. However, E_a values which were calculated with Ozawa, OFW and KAS method supports this suggestion. Average E_a values in Schiff base complex explosion reactions were, respectively, according to Ozawa method 134.59, OFW method 137.18 ± 19.57 kJ mol^{-1} and KAS method 135.16 ± 23.84 kJ mol^{-1}; however, these values in reduced Schiff base complexes were calculated, respectively, Ozawa method 126.94 kJ mol^{-1}, OFW method 125.15 ± 5.11 kJ mol^{-1} and KAS method 120.89 ± 6.22 kJ mol^{-1}. Standard deviations are higher, and E_a values which were calculated in reduced Schiff base complexes are lower as expected. But it is not possible to calculate this on explosion reactions clearly with these methods because TG curve shows anomaly. Tables 6 and 7 show the calculated thermodynamic parameters using the E_a and A values.

It was also considered that these complexes exhibit antimicrobial activity. To investigate the difference in biological activities for two different complex types, we

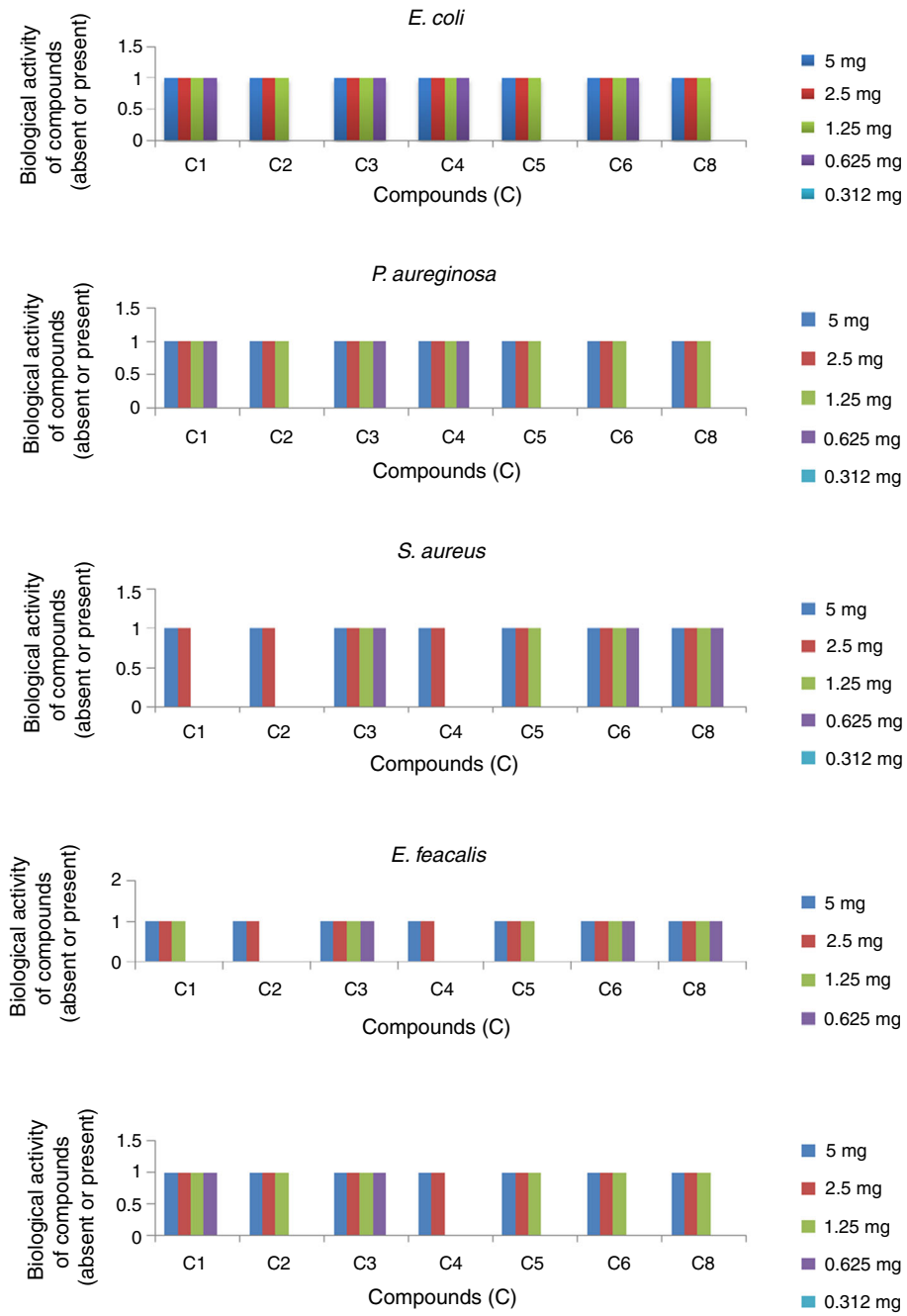

Fig. 16 Biological activity of the complexes prepared, C1, complex I; C2, complex II; C3, complex III; C4, complex IV; C5, complex VI; C6, complex VII and C8, complex IX

performed antibacterial and antifungal activity experiments. As mentioned above, inhibitory effects of these complexes analyzed against two gram-negative bacteria (*E. coli* and *P. aureginosa*), two gram-positive bacteria (*S. aureus* and *E. feacalis*) and one fungus (*C. albicans*). Results belonging to eight complexes against above-mentioned microorganisms are given in Fig. 16.

As shown in Fig. 16, there has been inhibitory effects observed against bacterial species and a fungus yet there is no significant difference between antibacterial and antifungal effects of both group of complexes. Thermokinetic results show that there is a small difference between two groups of complexes. But reaction that was examined with kinetic analysis is an explosion reaction. No doubt TG curve in explosion reactions was not good enough. Therefore, not observing a big difference in biological activity should be expected. If this study could be repeated with anions other than nitrate and nitrite anions, result would show clear comparison with respect to antimicrobial activity.

Conclusion

Totally eight trinuclear complexes were prepared from two different groups where nitrate and nitrite ions exist as μ-bridge and thermokinetic parameters were determined by four different methods isothermally and non-isothermally. Obtained data compared and stability among groups was researched. Small difference was determined between activation energies, but this difference was not calculated at biological activities. As a result, it was concluded that trinuclear complexes in some cases are more stable than mononuclear units.

References

1. Fukuhara C, Tsuneyoshi K, Matsumoto N, Kida S, Mikuriya M, Mori M. Synthesis and characterization of trinuclear Schiff-base complexes containing sulphur dioxide or hydrogensulphite ions as bridging groups. J Chem Soc Dalton Trans. 1990. doi:10.1039/DT9900003473.
2. Gerli A, Hagen KS, Marzilli LG. Nuclearity and formulation of $SALPN^{2-}$ complexes formed from $M(O_2CCH_3)_2$. Inorg Chem. 1991;30:4673–6.
3. Ülkü D, Tahir MN, Atakol O, Nazir H. Bis{(μ-acetato)[μ-bis(salicylidene)-1,3-propanediaminato)](*N*,*N*′-dimethylformamide)nickel(II)}cadmium(II). Acta Cryst. 1997;C53:872–4.
4. Ülkü D, Ercan F, Atakol O, Dinçer FN. Bis{(μ-acetato)[μ-bis(salicylidene)-1,3-propanediaminato)](dimethylsulphoxide)nickel(II)}nickel(II). Acta Cryst. 1997;C53:1056–7.
5. Uhlenbrock S, Wegner R, Krebs B. Syntheses and characterization of novel tri- and hexa-nuclear zinc complexes with biomimetic chelate ligands. J Chem Soc Dalton Trans. 1996. doi:10.1039/DT9960003731.
6. Atakol O, Nazir H, Aksu M, Arıcı C, Ercan F, Çiçek B. Some Di- and trinuclear zinc complexes: anion ınduced complex formation. Synth React Inorg Met Org Chem. 2000;30:709–18.
7. Ercan F, Atakol O. A linear trinuclear Ni^{II}–Mn^{II}–Ni^{II} complex with a μ-acetato bridge. Acta Cryst. 1998;C54:1268–70.
8. Ercan F, Atakol O, Arıcı C, Svoboda I, Fuess H. Tgree heteronuclear Schiff base complexes of nickel(II), with cobalt(II), copper(II) and manganese(II). Acta Cryst. 2002;C58:m193–6.
9. Sanmartin J, Bermejo MR, Garia-Deibe AM, Maneiro M, Lage C, Costa-Filho AJ. Mono and polynuclear complexes of Fe(II), Co(II), Ni(II), Cu(II), Zn(II) and Cd(II) with *N*,*N*′-bis(salicylidene)-1,3-dianino-2propanol. Polyhedron. 2000;19:185–92.
10. Shi DH, You ZL, Xu C, Zhang Q, Zhu HL. Synthesis, crystal structure and urease inhibitory activities of Schiff base metal complexes. Inorg Chem Commun. 2007;10:404–6.
11. Saha S, Sasmal A, Choudhury CR, Gomez-Garcia CJ, Garribba E, Mitra S. A new linear double bridged trinuclear Cu(II) Schiff base complex. Polyhedron. 2014;69:262–9.
12. Das LK, Kadam RM, Bauza A, Frontera A. Differences in nuclearity shapes and coordination modes of azide in the complexes of Cd(II) and Hg(II) with a metalloligand [CuL] (H_2L= *N*,*N*′-bis(salicylidene)-1,3-propanediamine). Inorg Chem. 2012;51:12407–18.
13. Hazari H, Ghosh A. Trinuclear complexes of [CuL] (H_2L=*N*,*N*′-bis(salicylidene)-1,4-butanediamine with HgX2 ($X=N_3^-$ and NCO^-). Polyhedron. 2015;87:403–10.
14. Biswas S, Ghosh A. Use of Cu(II)-di-Schiff bases as metalloligands in the formation of complexes with Cu(II), Ni(II) and Zn(II) perchlorate. Polyhedron. 2013;65:322–31.
15. Arıcı C, Ülkü D, Atakol O. Bis{(*N*,*N*′-dimethylformamide) (μ-formato)[μ-bis(salicylidene)-1,3-propanediaminato)] nickel(II)}-cobalt(II). Anal Sci. 2002;18:959–60.
16. Ercan F, Ateş BM, Durmuş S, Atakol O. Structural analysis of bis{(B,*N*'-dimethylformamide)(μ-formato)[μ-bis(salicylidene)-1,3-propanediaminato]nickel(II)}copper(II) and zinc(II) monohydrate hetero-trinuclear complexes. Cryst Res Tecnol. 2004;39:470–6.
17. Chen YN, Ge YY, Zhou W, Fang L, Gu ZG, Ma GM, Li WS. The first Mn–Zn heterometallic dinuclear compound based on Schiff base ligand *N*,*N*′-bis(salicylidene)-1,3-propanediamine. Inorg Chem Commun. 2011;14:1228–32.
18. Akay A, Arıcı C, Atakol O, Fuess H, Svoboda I. Synthesis, crystal structure and thermoanalysis of bis {[μ-bis-*N*,*N*′(2-hydroxybenzoyl)-1,3-propandiaminato](*N*,*N*′-dimethylformamide)(μ-benzoato) nickel(II)} nickel(II). J Coord Chem. 2006;59:933–8.
19. Atakol O, Tatar L, Akay MA, Ülkü D. Crystal structure of trinuclear complex, Bis[μ-*N*,*N*′-bis(salicylidene)1,3-propanediaminato(dimethylformamide)(μ-nitrito)nickel(II)]cobalt(II). Anal Sci. 1999;15:101–2.
20. Atakol O, Arıcı C, Tahir MN, Kurtaran R, Ülkü D. Crystal structure of Bis[μ-*N*,*N*′-bis(salicylidene)1,3-propanediaminato(dimethylformamide)(μ-nitrato)nickel(II)]nickel(II). Dimethyl formamide solvate. Anal Sci. 1999;15:933–4.
21. Yıldırım LT, Atakol O. Crystal structure analysis of Bis {(*N*,*N*′-dimethylformamide)-[μ-bis-*N*,*N*′(2-oxybenzyl)-1,3-propanediaminato](μ-acetato) nickel(II)}nickel(II). Cryst Res Technol. 2002;37:1352–9.
22. Reglinski J, Taylor MK, Kennedy AR. Hydrogenated Schiff base ligands. Inorg Chem Commun. 2006;9:736–9.
23. Kurtaran R, Yıldırım LT, Azaz AD, Namlı H, Atakol O. Synthesis, characterization, crystal structure and biological activity of a novel heterotetranuclear complex. J Inorg Biochem. 2005;99:1937–44.
24. Mustapha A, Busche C, Reglinski J, Kennedy AR. The use of hydrogenated Schiff base ligands in the synthesis of multi metallic compounds II. Polyhedron. 2011;30:1530–7.
25. Song Y, Gamez P, Roubeay O, Mutikainen I, Turpeinen U, Reedijk J. Structure and magnetism of two new linear trinuclear copper(II) clusters obtained from the tetradentate N_2O_2 ligand bis(2-hydroxybenzyl)-1,3-diaminopropane. Inorg Chim Acta. 2005;358:109–15.
26. Aksu M, Durmuş S, Sarı M, Emregül KC, Svoboda I, Fuess H, Atakol O. Investigation on the thermal decomposition some heterodiniclear Ni^{II}–M^{II} complexes prepared from ONNO type reduced Schiff Base compounds (M^{II}=Zn^{II}–Cd^{II}). J Therm Anal Calorim. 2007;90:541–7.
27. Öz S, Titiš J, Nazır H, Atakol O, Boca R, Svoboda I, Fuess H. Synthesis, structure and magnetic properties of Ni(II)–Co(II) heterodinuclear complexes with ONNO type Schiff bases as ligands. Polyhedron. 2013;59:1–7.
28. Durmuş S, Ergun Ü, Jaud JC, Emregül KC, Fuess H, Atakol O. Thermal decomposition of some linear trinuclear Schiff base complexes with acetate bridges. J Therm Anal Calorim. 2006;86:337–46.
29. Ozawa T. Kinetic analysis of derivative curves in thermal analysis. J Therm Anal. 1970;2:301–24.
30. Koga N. Ozawa's kinetic method for analysing thermoanalytical curves. J Therm Anal Calorim. 2013;113:1527–41.
31. Ledeti I, Fuliaş A, Vlase G, Vlase T, Bercean V, Doca N. Thermal behaviour and kinetic study of some triazoles as potential anti-inflammatory agents. J Therm Anal Calorim. 2013;114:1295–305.

32. Abdel-Kader NS, Amin RM, El-Ensary AL. Complexes of Schiff base of benzopyran-4-one derivative. J Therm Anal Calorim. 2016;123:1695–706.
33. Zziana A, Vecchio S, Gdaniee M, Czapik A, Hadzidimitriou A, Lalia-Kantouri M. Synthesis, thermal analysis, and spectroscopic and structural characterizations of zinc(II) complexes with salicylaldehydes. J Therm Anal Calorim. 2013;112:455–64.
34. Kullyakool S, Danvirutai C, Siriwong K, Noisong P. Determination of kinetic triplet of the synthesized $Ni_3(PO_4)_2.8H_2O$ by non-isothermal and isothermal kinetic methods. J Therm Anal Calorim. 2015;115:1497–507.
35. Koyundereli-Çılgı G, Çetişli H, Donat R. Thermal kinetic analysis of uranium salts. J Therm Anal Calorim. 2014;115:2007–20.
36. Krajnikova A, Rotaru A, Györyova K, Homzova K, Manolea HO, Kovarova J, Hudecova D. Thermal behaviour and antimicrobial assay of some new zinc(II) 2-aminobenzoate complex compound with bioactive ligands. J Therm Anal Calorim. 2015;120:73–83.
37. Sarada K, Muraleedharam K. Effect of addition of silver on the thermal decomposition kineticsw of copper oxalate. J Therm Anal Calorim. 2016;123:643–51.
38. Ebrahimi HP, Hadi JS, Abdulnabi ZA, Bolandnazar Z. Spectroscopic, thermal analysis and DFT computational studies of Salen type Schiff base complexes. Spectrochim Acta A. 2014;117:485–92.
39. Soliman AA, Linert W. Investigations on new transition matal chelates of 3-methoxy-salicylidene-2-aminothiophenol Schiff base. Thermochim Acta. 1999;338:67–75.
40. Oxford Diffraction CrysAlis CCD and CrysAlis RED. Version 1.170.14. Oxfordshire: Oxford Diffraction; 2002.
41. Sheldrick GM. SHELXS_97 and SHEXL_97, program for crystal structure solution and refinement. Göttingen: University of Göttingen; 1997.
42. Farrugia LJ. WinGX suite for small-molecule single-crystal crystallography. J Appl Cryst. 1999;32:837–8.
43. Atakol O, Nazir H, Arıcı C, Durmuş S, Svoboda I, Fuess H. Some new Ni–Zn heterodinuclear complexes: square-pyramidal nickel(II) coordination. Inorg Chim Acta. 2003;342:295–300.
44. Öz S, Arıcı C, Emregül KC, Ergun Ü, Atakol O, Kenar A. Heteronuclear Ni(II)–Sn(II) complexes from reduced ONNO type Schiff base compounds. Z Kristallogr. 2007;222:249–54.
45. Klapötke TM. Chemistry of high-energy materials. Berlin: Walter de Gruyter; 2011. p. 38.